

# A Study on Microstructure of Functionally Graded Composite Steels for Lead-bismuth cooled Fast Reactor Cladding Application

Jeonghyeon Lee, Taeyong Kim and Ji Hyun Kim\*

Department of Nuclear Engineering, School of Mechanical, Aerospace and Nuclear Engineering, Ulsan National Institute of Science and Technology (UNIST)

\*kimjh@unist.ac.kr

## 1. Introduction

Liquid metal coolants such as lead, lead-bismuth eutectic (LBE), and sodium also have the benefits of higher thermal conductivities and heat capacities than most other coolants. The advantages of lead or lead-bismuth eutectic, which has attractive thermal, hydraulic, and nuclear-physics properties, make these coolants ideal for fast-reactor and accelerator-target applications. However, at temperatures of interest for advanced reactor applications (>500 °C), such as high-efficiency electricity generation or producing process heat for high temperature electrolysis, the corrosion of cladding and structural materials becomes the limiting factor.

Heavy liquid metals are adequate for transmutation of nuclear waste and spent fuel, as their heavy nuclei make it possible to obtain a very fast neutron spectrum, and nuclear safety and nuclear waste problems are important issues to consider. Long-lived minor actinides, such as neptunium or americium, which occur in nuclear waste, can be burned.

The weld overlay technique is a widely used approach in nuclear industries; light water reactors typically use this hybrid layer technique in pressure vessels and fuel cladding. Pressure vessels are usually made of carbon steels, which will endure the pressure. Weld overlaying of stainless steel inside the pressure vessel serves as a corrosion-resistant layer for the vessel [1]. In fuel cladding tubes, which hold the fissile fuel in a core, pure zirconium is clad inside a zirconium alloy such as Zircaloy and advanced zirconium [2, 3]. The pure zirconium serves as the corrosion-resistant layer, while the zircaloy serves as the structural layer. Occasionally, the zirconium liner on the inside of this type of fuel cladding, known as a fuel barrier, helps prevent fuel-cladding interactions. These approaches are not suitable for fast reactor applications.

Nuclear reactor cladding tubes are manufactured using the extrusion, drawing, and pilgering process, which is commonly known as a manufacturing process [4, 5]. Pilgering is a cold working operation where the outside diameter, inside diameter, and wall thickness of tubes are simultaneously reduced over the working length under a pair of dies with semi-circular tapered grooves cut on them [6]. Pilgering is often characterized by a Q-factor that is the ratio of the strain due to change in thickness to the strain resulting from reduction in

diameter of the tube. It has been found that there is an improvement in the quality of the final product with increase in Q value (Ref.7). The Q ratio is variously defined as

$$Q = \frac{\Delta t/t_0}{\Delta D/D_0} = \frac{\Delta t/t_0}{\Delta D_{MW}/D_{0MW}} \quad (1)$$

where  $t$  is the thickness,  $D$  is the diameter and the subscript refers to the original or starting values. The right-hand side of the above equation with subscripts MW specifies mid-wall.

The goal of this paper is to further develop the functionally graded metallic composite. This functionally graded metallic composite will ultimately be available to be used as piping and fuel cladding in a lead-bismuth cooled nuclear reactor. The tasks provide a detailed description of the work completed within this paper. One of the work is to complete a detailed microstructural analysis of the piping product using optical microscopy. The second one is to optimize the microstructure and mechanical properties of the T91 and Fe-12Cr-2Si layers in the piping product through heat treatment.

## II. EXPERIMENTAL AND METHODOLOGY

### II.A. Selection of Composite Materials

Lim et al. proposed the Fe-Cr-Si alloy system as a high-temperature, corrosion-resistant material. From corrosion tests with a series of alloys based on the Fe-Cr-Si system, it has been verified that Fe alloys with suitable levels of Cr (>12 wt%) and Si (>2.5 wt%) will be protected by either a tenacious oxide film (over a wide range of oxygen potentials above the formation potential for Cr and Si oxides) or by a low solubility surface region at low oxygen potentials. Experimental results obtained from model alloys after LBE exposure at 600 °C demonstrated the film formation process. The hypothesis that Si addition would promote the formation of a diffusion barrier was confirmed by the actual reduction of oxide thickness over time. The Si effect was enhanced by the addition of Cr to the system [6].

Based on their extensive characterization study, they proposed the concept of an FGC consisting of two layers, a thin Fe-12Cr-2Si layer as a corrosion-resistant

layer and T91—chosen for its strength and radiation resistance—as a structural layer [7]. Also, other ferritic/martensitic steels, like HT9 or Gr.92, can be

Table 1. Chemical composition of Fe-12Cr-2Si weld wire and T91 in wt.%

	Fe	Cr	Mn	Mo	Ni	Si	V	W	N	C
T91	Bal.	9.4	0.51	1.0	0.28	0.35	0.19	0.07	-	-
Fe-12Cr-2Si	Bal.	13.11	0.02	-	0.006	2.0	-	0.17	-	0.01

selected for structural layer materials for various reactor applications. HT9 and Gr.92 have already showed good mechanical properties in a high-temperature sodium environment (Ref.8). Table 1 shows the chemical compositions of Fe-12Cr-2Si and T91 steels.

### II.B. Hot extrusion and Cold Pilgering

The hot extrusion process was performed at MIT. The composite design consists of an T91 base structural layer with a Fe-12Cr-2Si corrosion resistant barrier. The weld wire from the Fe-12Cr-2Si was overlaid on the long cylindrical billets of T91 steel which is 23.4 cm outer diameter and 60.9 cm length. For the fuel cladding the Fe-12Cr-2Si weld wire was weld overlaid on the outer diameter of the T91 cylindrical billet that had been center drilled. These billets were then extruded into Tube Reduced Extrusions (TRES) 9.52 cm (3.75") OD 518 cm (408") long (TRES) tubing at ~1200 °C.

The cold pilgering test of the tube was conducted using the reducing schedule below, and the reduction rate of first pilgering in area is 53%. Reduction rate was maintained under the 60% for the safe process. And the Q factor of first pilgering was set as 1.58 for the similar value. Those factors are reviewed by the Korea Institute of Materials Science.

The procedure of manufacturing of FGC tube consists of 3 steps. The first scheme is the overlay welding the Fe-12Cr-2Si to the T91. The choice of T91 as a structural layer in the composite was originally based on material availability. The purpose of the development effort was to take corrosion off the issue so that future versions of the composite might use a higher strength alloy. It has also been shown that for a fractured pipe one will see no dis-bonding between the Fe-12Cr-2Si layer and the T91 layer. This task was performed at MIT. The second scheme was a hot extrusion. The hot extrusion process of the FGC tube is manufactured from the mechanically FGC billet. And the final scheme was a cold pilgering to FGC tube for reducing the tube size. The 1<sup>st</sup> step of pilgering was performed recently. And the next step of pilgering will be performed, sequentially.

The cold pilgering test is performed using a typical 125 VMR type mill manufactured by Manesmann Meer. A feed step of 3 mm per stroke cycle was used for all case of pilgering process. And the stroke rate is 30 stroke per minute.

## III. RESULTS AND DISCUSSION

### III.A. Microstructure after hot extrusion

Fig. 2 shows the optical microscopy result of FGC tube after the hot extrusion including the microstructure of Fe-12Cr-2Si materials on the T91 cladding and the out surface of cladding. The thickness of Fe-12Cr-2Si layer is 1500 μm (1.5mm). In the inner part, Ferritic/martensitic phase was observed. And, austenitic grain boundary at Fe-12Cr-2Si was observed. Extrusion forming involves placing billet into a container and then applying pressure to them cause plastic deformation. Materials with small grain size has an increased yield strength, higher ultimate strength, according to Hall-Petch strengthening.

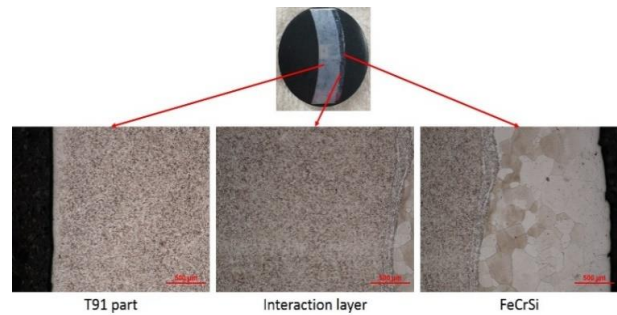


Fig. 1. Microstructure after hot extrusion

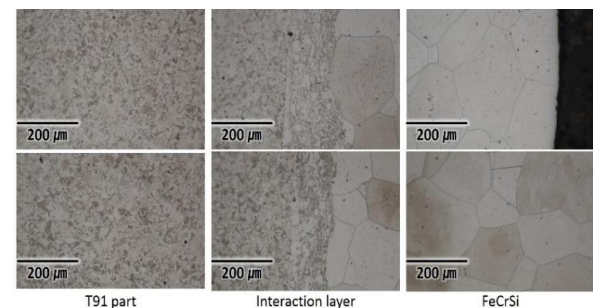


Fig. 2. Microstructure of FGC tube after hot extrusion

During the hot deformation process, the flow stress is sensitive to the work hardening and the dynamic softening. At the beginning of the deformation, the flow stress increases with the increasing strain. The material is under an unstable status due to the increasing dislocation density. The stored energy turns into a driving force for the dislocation migration. When the strain reaches to the critical strain, the dynamic recovery occurs and the flow stress increases owing to the conffliction between softening and hardening. Moreover, with the strain continuing to increase, the work hardening and softening reach to a certain balance and the flow stress reaches to a plateau as well. Thus, the critical strain and work hardening are the significant parameters for the flow stress and should be considered in the constitutive models.

### III.B. Crack examination after hot extrusion

The FGC billet was then preheated to 816 °C in a reducing gas furnace for one hour, followed by an induction preheat to between 1,193 and 1,224 °C for 15 minutes. The billet was then immediately rolled out of the furnace and onto a fiberglass blanket. Glass lubricant was poured into the inner diameter, glass endcaps were melted on, and the billet was extruded within 15 seconds.

Fig. 3 shows the microstructure of Fe-12Cr-2Si materials on the FGC cladding with a small amount of intergranular pores tend to be more prone to grain boundary cracking after hot extrusion processing.

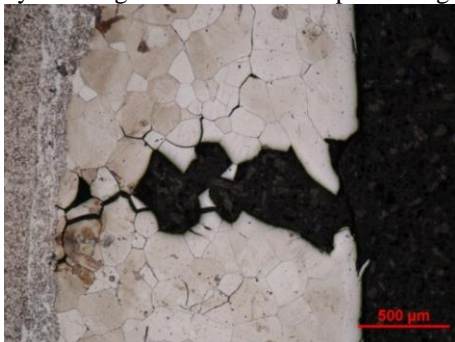


Fig. 3. Microstructure of crack on Fe-12Cr-2Si

There are many reasons for the surface cracking during the hot extrusion processing which are i) grain boundary segregation ii) surface cracking by hot extrusion iii) hot cracking iv) reheat cracking by welding and extrusion v) crack of overlay weld metal by residual stress.

To investigate the near crack zone in specimens that were exposed to hot extrusion, electron probe micro analyzer X-ray mapping was also used. In fig. 4, scattered electron (SE) image shows the specimen (excluding the left margin, which is the mounting resin containing O and C). In the image from the Cr and Si X-ray peak, those elements were enriched by the hot extrusion.

According to S. Hofmann et al., the temperature dependencies of silicon segregation to two grain boundaries exhibit a maximum near 627 °C (Ref.9). In the bicrystalline steel (Fe-Si steel), it has {112} and {013} symmetrical grain boundaries. Both the decrease of silicon segregation at 500 °C and a relatively wide in-depth range of the silicon enrichment at all temperatures independent of the values of diffusion length estimates, are found for both grain boundaries. The annealing temperatures and times are presented in table 2.

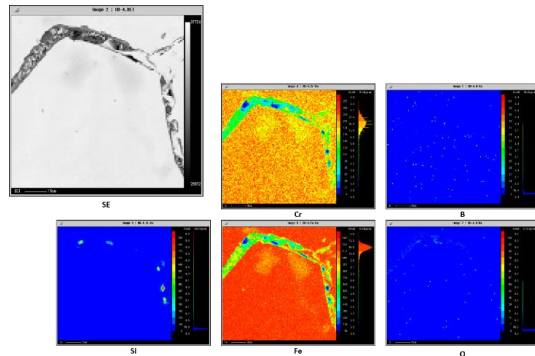


Fig. 4. Microstructure of crack on Fe-12Cr-2Si

TABLE 2. Values of silicon diffusivities were calculated from data of Si diffusion from data<sup>9</sup>.

Temperature (K)	1173	1073	973	873		773		
Time, t (h)	24	24	48	96	120	168	240	1440
$\sqrt{D_{Si}t}$ (μm)	89	34	15	5	6	1	1.4	3.5

Surface cracking from high work-part temperatures that causes crack to develop at the surface. They often occur when extrusion speed is too high, leading to high strain rates and associated heat generation. Both solidification cracking and hot cracking refer to the formation of shrinkage cracks during the solidification of weld metal, although hot cracking can also refer to liquation cracking. The cracking which occurred in the heat material was located exclusively at grain boundaries. Further, temperature variations across the billet during hot extrusion can also lead to inhomogeneous deformation.

### III.C. Effect of heat treatment for FGC tube

The residual stress of the process finished FGC tubes was determined by the Sachs method; the process FGC tube exhibited changing residual stress across the wall thickness and tensile and compressive stresses near the outer and inner sides.

The Vickers hardness of the FGC tube will be subjected to heat treatment and cold pilgering will be measured at a load of 10 N; the hardness will be measured using a HM-220 hardness testing machine.

The extrusion process was stopped before the ram reached the dead zone. In order to study the effect of the hot extrusion process on the extruded material hardness, Vickers hardness will be measured in dead and extruded zones for samples of each steps.

According to Westbrook (Ref.10), the temperature dependence of hardness of metals and alloys has been reviewed. The summary of his equation for hardness by temperature is that the temperature dependence of hardness is best represented by the following relation of the type

$$H = A \exp(-BT) \quad (2)$$

where constants  $A$  and  $B$  are called the intrinsic hardness (i.e. the value of hardness at 0 K) and softening coefficient, respectively. The specimen of hardness will be analyzed until conference.

The heat treatment affects the carbide/precipitation phases and microstructures such as type, size, and volume of defects. It is play a decisive role in changing the mechanical properties such as hardness, creep property, and strength. According to literature, the austenite grain and ferrite grain might change at temperature higher than 1150 °C because of the dissolution of carbide and precipitation in alloy steel. Heat treatment can be improved removing of carbide/precipitation. Precipitation removes these materials from solid solution, and thus those things no longer available for interaction crack and solid solution hardening. The heat treated specimen will be analyzed until conference

Precipitation removes these species from solid solution, and thus they are no longer available for interaction solid-solution hardening.

#### IV. CONCLUSION

The functionally graded metallic composite will ultimately be available to be used as piping and fuel cladding in a lead-bismuth cooled nuclear reactor. The tasks provide a detailed description of the work completed within this paper. It has been completed a detailed microstructural analysis of the piping product using optical microscopy. Although the solution-precipitation reaction is fundamentally reversible with temperature change, in many alloys transition structures form during precipitation but not during solution.

Main results are as follows:

i) The results were noticed that microstructure of Fe-12Cr-2Si materials on the FGC tube with small amount of intergranular pores tend to be more prone to grain boundary cracking after hot extrusion processing

ii) There are key factors for cracking at overlay weld materials. Surface cracking is closely related to the

temperature rise during extrusion. Hot cracking is the reason of cracking in Fe-12Cr-2Si weldment.

iii) After the heat treatment, the Si phase grows to granular grain, so that the stress contraction can be avoided, which eliminated the tearing effect on the matrix.

To optimize for manufacturing process of cladding tube, it is important to identify and resolving problem each step of manufacturing process. If the problems of each process can be solved, mass production of FGC cladding tube will be possible. The crack on surface of tube can be solved by heat treatment and cold pilgering process.

And the cold pilgering is under process and the microstructure change has been analyzed. Also, the hardness will be measured using a HM-220 hardness testing machine. This result will be updated at final paper for the conference.

#### ACKNOWLEDGMENTS

This work was supported by the National Nuclear R&D program funded by Ministry of Science, ICT and Future Planning, and by the National Nuclear R&D program organized by the National Research Foundation (NRF) of South Korea in support of the Ministry of Science, ICT and Future Planning.

#### REFERENCES

1. J. Lim, H.O. Nam, I.S. Hwang, and J.H. Kim, *Journal of Nuclear Materials*, 407, 205 (2010)
2. N.P.Gurao, H. Akhiani, J.A. Szpunar, *Journal of Nuclear Materials*, 453, 158 (1967)
3. P. Platt, V. Allen, M. Fenwick, *Corrosion Science*, 98, 1 (2015)
4. E. Vanegas-Márquez, K. Mocellin, L. Toulbi, Y. de Carlan, and R.E. Logé, *Journal of Nuclear Materials*, 420, 479 (2012)
5. K. Linga Murty, and I. Charit, *Progress in Nuclear Energy*, 48, 325 (2006)
6. G. Müller, G. Schumacher, D. Strauß, *Surface and Coatings Technology*, 135, 196 (2001)
7. A. Weisenburger, A. Heinzl, G. Müller, H. Muscher, and A. Rousanov, *Journal of Nuclear Materials*, 376, 274 (2008)
8. A. Heinzl, M. Kondo, and M. Takahashi, *Journal of Nuclear Materials*, 350, 264 (2006)
9. S. Hofmann, P. Lejck, *Journal de Colloques*, 51 (1990) C1-179
10. J. H. Westbrook et al., *Trans. Am. Soc. Met.* 45 (1953) 221.